

## Reconstructing fluctuations of a shallow East African lake during the past 1800 yrs from sediment stratigraphy in a submerged crater basin

Dirk Verschuren

*Limnological Research Center, University of Minnesota, Minneapolis, MN 55455, USA & Department of Biology, Ghent University, Ledeganckstraat 35, B-9000 Gent, Belgium (E-mail: dirk.verschuren@rug.ac.be)*

Received 28 April 1999; accepted 7 January 2000

**Key words:** Africa, diatom mats, lake level, Little Ice Age, Mediaeval Warm Period, organic carbon, paleoclimate, sedimentology

### Abstract

The sedimentology of an 8.22-m long core of late-Holocene deposits in the submerged Crescent Island Crater basin of Lake Naivasha, Kenya, is used to reconstruct decade-scale fluctuations in lake-surface elevation during the past 1800 yrs. Lake-depth inference for the past 1000 yrs is semi-quantitative, based on (1) relationships between lake level and bottom dynamics predicted by wave theory, and (2) historical validation of the effects of lake-level fluctuation and hydrologic closure on sediment composition in Crescent Island Crater and nearby Lake Oloidien. In these shallow fluctuating lakes, organic-carbon variation in a lithological sequence from clayey mud to algal gyttja is positively correlated with lake depth at the time of deposition, because the focusing of oxidized littoral sediments which dilute autochthonous organic matter before burial is reduced during highstands. The lake-level reconstruction for Lake Naivasha agrees with other adequately dated lake-level records from equatorial East Africa in its implication of dry climatic conditions during the Mediaeval Warm Period and generally wet conditions during the Little Ice Age. Crescent Island Crater survived widespread aridity in the early-19th century as a fresh weedy pond, while the main basin of Lake Naivasha and many other shallow East African lakes fell dry and truncated their sediment archive of Little Ice Age climatic variability.

### Introduction

The last few thousand years of the climate history of East Africa, and specifically the regional patterns and magnitude of climatic variability during the Mediaeval Warm Period (MWP~AD 1000–1300) and Little Ice Age (LIA~AD 1300–1850), are still poorly understood. The handful of existing high-resolution climate-proxy records all suggest that this period witnessed a succession of century-scale climate shifts, but poor chronological control precludes evaluation of the spatial coherence of these climatic anomalies across East Africa, or correlation with contemporaneous climate shifts documented from temperate latitudes. Records from Lake Victoria (Stager et al., 1997) and Lake Malawi (Owen et al., 1990), and reconstructions of past veg-

etation in Ethiopia (Bonnefille & Mohammed, 1994), seem to indicate that equatorial East Africa was significantly drier than today for most of the period between about AD 1400 and 1850. In contrast, records from Lake Turkana (Halfman et al., 1994) and Lake Tanganyika (Cohen et al., 1997) infer a relatively dry MWP but significantly wetter conditions from about AD 1250 to at least 1600. Evidence of pronounced LIA-period highstands also occurs in several of the (typically incomplete) records from shallow fluctuating lakes in the region, for example during AD 1650–1760 at Lake Chilwa in Malawi (Owen & Crossley, 1989) and during AD 1570–1800 at Lake Chad in the Sahel (Maley, 1976). The apparent conflict between these two sets of records is troubling because the inferred magnitude of LIA-period lake fluctuation is substantially

larger than that recorded during historical times, seeming to imply large and sustained rainfall anomalies that can not be attributed to local climatic contrasts.

To evaluate the regional coherence of decade- to century-scale climate shifts, a network of lake-sediment records is needed that are all certain to represent a continuous archive of local climate history over the last few thousand yrs, and can be meaningfully resolved at a time scale of decades. In East Africa it has been difficult to find suitable study sites because lakes with adequate hydrological sensitivity to create a climate-proxy record with decade-scale signal resolution tend to be subject to intermittent complete desiccation, and the truncation or partial loss of that record, over longer time periods (Verschuren, 1999a). The need for long climate-proxy records with good time resolution places a premium on methods that inexpensively and quickly assess both archival quality and the relative magnitude of system response to decade-scale climate shifts, before major effort goes into costly and labor-intensive analyses of geochemical and biological climate-proxy indicators. Previous work on Lake Naivasha in central Kenya (Verschuren, 1999a) showed how empirical relationships between basin morphometry and bottom dynamics (Håkanson, 1977, 1982; Hilton, 1985) can be used to predict the effects of past lake-level fluctuation on the integrity and time resolution of sedimentary climate-proxy records. This study uses the historical sedimentation patterns in two of Lake Naivasha's four basins to investigate the effects of lake-level fluctuation and hydrological closure on the composition of offshore sediments. The observed relationships are then applied to the sediment characteristics of an 8.22-m long sediment core from near the deepest point of Lake Naivasha's Crescent Island Crater basin to reconstruct decade- to century-scale lake-level changes over the past 1800 yrs.

### Study area

Lake Naivasha and its satellite basins Crescent Island Crater, Lake Oloidien, and Lake Sonachi are located at about 1885 m above sea level (a.s.l.) in the central valley of the Eastern Rift in Kenya (Figure 1). Much of the monsoonal rainfall in the region is intercepted by surrounding highlands, creating a strong moisture deficit near the lakes with annual rainfall and evaporation averaging 608 and 1865 mm (Åse et al., 1986). The main basin of Lake Naivasha is a large (135 km<sup>2</sup> in 1993), shallow (6 m), and wind-stressed

freshwater lake. Its catchment (2378 km<sup>2</sup>) is topographically closed, but hydrologically open with groundwater flowing towards the lake from the north and exiting in the south and southeast (Gaudet & Melack, 1981). At its current level, the lake's residence time is on the order of 6 yrs (Ojiambo & Lyons, 1996). Crescent Island Crater is a small (1.9 km<sup>2</sup>) and deep (16 m), submerged crater basin near the east shore of Lake Naivasha. It is hydrologically open due to confluence with the main basin and groundwater throughflow. Lake Oloidien (5.1 km<sup>2</sup>) is shallow and hydrologically closed, and Lake Sonachi (0.14 km<sup>2</sup>) is a saline crater lake maintained by groundwater flow from Lake Naivasha (MacIntyre & Melack, 1982). The combined Lake Naivasha system is maintained by river input primarily from the Malewa River, which drains the wet Nyandarua Range and Kinangop Plateau to the east. The Lake Naivasha water budget is dominated by evaporation from the lake surface (80% of total loss) and strongly variable river inflow (on average 56% of total input), so that lake level fluctuates as in a hydrologically closed system (Gaudet & Melack, 1981; Darling et al., 1990). Over the past 115 yrs, the depth of Crescent Island Crater has varied between a high of 27 m in 1894 and a historic low of 12 m in 1946. Although the crater at this time was almost completely separated from a much reduced Lake Naivasha (cf. the 5-m depth contour in Figure 1), solute removal through subsurface outflow maintained freshwater conditions (Verschuren, 1996). In contrast, separation of Lake Oloidien from Lake Naivasha during the mid-20th century lowstand resulted in evaporative concentration of dissolved salts because Lake Oloidien depends on surface confluence with Lake Naivasha to remain fresh (Verschuren et al., 1999). When Crescent Island Crater is confluent with Lake Naivasha, it functions as a sediment trap for clastic input from the shallow, wind-stressed northeast sector of Lake Naivasha (Figure 1). This results in an uncommonly high rate of sediment accumulation on the crater floor, which in turn enhances the time resolution of its sediment record by limiting the influence of physical and biological disturbance. At least 28 m of sediments have accumulated in Crescent Island Crater during the Holocene (Richardson & Richardson, 1972), about 1.20 m of which since European discovery of the lake in AD 1883 (Verschuren, 1999a).

### Methods

The studied material includes a short core (NC93.1-S: 0–122 cm) and a long core (NC93.2-L: 124–822 cm)

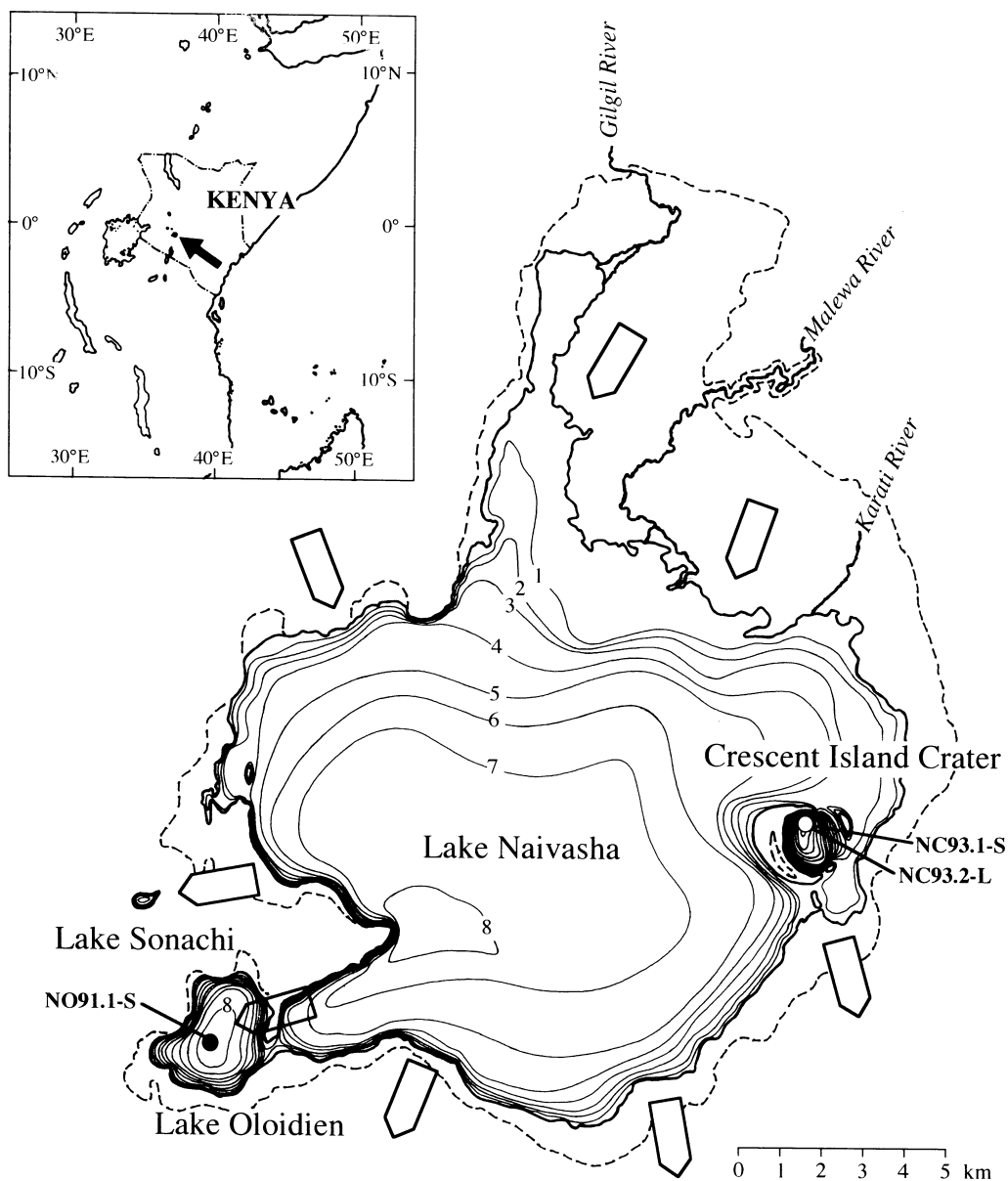


Figure 1. Location map of East Africa, bathymetry of Lake Naivasha and its satellite basins Crescent Island Crater, Lake Oloidien, and Lake Sonachi (in 1983, at 1886 m a.s.l.) with core sites, and the 1900 m a.s.l. contour as indication of minimum lake-surface area during the AD 1680–1770 highstand. Modified from Åse et al. (1986); white arrows show the direction of groundwater flow as in Gaudet & Melack (1981).

retrieved in 15.35 m water near the deepest point of Crescent Island Crater, and a second short core (NO91.1-S: 0–92 cm) retrieved in 6.15 m water near the center of Lake Oloidien (Figure 1). Both short cores were collected with a single-drive piston corer (Wright, 1980) and extruded upright in the field with a fixed-interval sectioning device (Verschuren, 1993); the long core was recovered in 1-m segments with a square-rod

piston corer (Wright, 1967), extruded in the field and wrapped in plastic and aluminium foil for transport.

The stratigraphy of each extruded core was described by color and texture. The weight fractions of organic matter (OM), carbonate ( $\text{CaCO}_3$ ), and non-carbonate inorganic matter in contiguous 1- or 2-cm core increments were determined by the loss-on-ignition (LOI) method of drying at 105 °C, burning at 550 °C,

and ashing at 1000 °C (Dean, 1974). Total carbon (TC) and inorganic carbon (IC) in 44 selected samples were measured with an IUC carbon analyzer; organic carbon (OC) was calculated by subtracting %IC from %TC. Strong correlations between %OM determined by weight loss at 550 °C and %OC determined by coulometry, and between %CaCO<sub>3</sub> determined by weight loss at 1000 °C and %IC determined by coulometry, indicate that composition data obtained by LOI are representative. Linear regression of %OC over %OM yielded the equation  $\%OC = 0.533 * \%OM - 1.012$  ( $r^2 = 0.94$ ;  $n = 44$ ); linear regression of %IC over %CaCO<sub>3</sub> yielded  $\%IC = 0.111 * \%CaCO_3 - 0.352$  ( $r^2 = 0.93$ ;  $n = 44$ ). The intercept value of 3.2% CaCO<sub>3</sub> at 0% IC represents the average weight loss at 1000 °C that can be attributed to removal of water bound to clay lattices (Dean, 1974). Weight fractions of medium-to-coarse sand and OM (> 250 µm; coarse OM is derived from aquatic macrophytes and swamp vegetation) were quantified by dispersing the sediment in 0.25% Calgon™, rinsing through a 250-µm sieve, and transferring the retained residue to ashless filter paper for analysis by LOI (Digerfeldt, 1986). Solid-phase biogenic silica (BSi) was determined by wet alkaline extraction (DeMaster, 1981), using a 0.5 M NaOH solution for sample digestion. Smear slide analysis was used to visually inspect grain-size variation in the mineral fraction of the sediment, and to confirm that algal production is the main source of fine OM. A distinct type of compact, diatom-rich sediment was also studied by scanning electron microscopy (S.E.M.).

The chronology of both short cores was determined by <sup>210</sup>Pb dating (Verschuren, 1999a). Pb-210 activity was measured through its granddaughter product <sup>210</sup>Po, with <sup>208</sup>Po added as an internal yield tracer. Supported <sup>210</sup>Pb activity was estimated as the asymptote of total activity at depth, and unsupported activity was calculated by subtracting average supported activity from total activity measured at each level. Sediment age at depth and accumulation rates were calculated with the c.r.s. (constant rate of supply) model (Appleby & Oldfield, 1978). The sediment chronology of Lake Oloidien history is anchored in four stratigraphic marker horizons for which the <sup>210</sup>Pb-inferred age matches their known or estimated age (Verschuren, 1999a; Verschuren et al., 2000). Pb-210 dating of core NC93.1-S proved problematic, possibly because the assumption of constant <sup>210</sup>Pb flux required by the c.r.s. model is violated by a strong dependence of sediment focusing into Crescent Island Crater on the degree of

its confluence with Lake Naivasha. The chronology presented here is based on plant macrofossil evidence reflecting three known outbreaks of the exotic water fern *Salvinia molesta* in 1969, 1982, and 1989 (Harper et al., 1990), and three other stratigraphic marker horizons that NC93.1-S has in common with a dated core from Lake Naivasha (Verschuren, 1999a; see also below). Downcore variation in residual <sup>210</sup>Pb activity, i.e. the deviation of <sup>210</sup>Pb concentrations from pure exponential decline with depth, is used as a proxy for the rate of sedimentation (Appleby & Oldfield, 1978). The chronology of pre-20th century deposits in core NC93.2-L is based on fourteen AMS <sup>14</sup>C dates obtained on individual plant macrofossils from discrete depth levels or on grass charcoal recovered by sieving larger core sections (Table 1). Agreement between the <sup>14</sup>C ages of emergent aquatic vegetation ( $1040 \pm 50$  <sup>14</sup>C yr BP) and terrestrial plant material ( $1030 \pm 50$  <sup>14</sup>C yr BP) from the depth interval 562–566 cm suggests that dates obtained on these different materials are interchangeable. The chronology of Crescent Island Crater history presented here combines the historical chronology for core NC93.1-S with ten <sup>14</sup>C dates from between 150 and 822 cm core depth in NC93.2-L (Figure 2). Radiocarbon ages were converted to calendar ages with the bidecadal calibration curve (Stuiver & Reimer, 1993). In cases where conversion yielded non-unique calendar ages, a 4th-order polynomial regression of all retained dates was used to determine the most probable calendar age corresponding with each <sup>14</sup>C date based on minimization of variation in sedimentation rate, after which core chronology was constructed by linear interpolation between these most-probable ages (Figure 2).

## Results

### *Relationships between lake level and sedimentation*

Variation in the color, texture, and organic-matter content of late-Holocene deposits in Crescent Island Crater allowed distinction of seven sediment types: algal gyttja, organic clayey mud, clayey mud, low-organic clayey mud, high-carbonate clayey mud, silty peat, and a compact diatom-rich material that occurs as discrete 1–6 cm thick layers ('diatom mats') within sections of the other sediment types. Composition data (Figure 3) show the sequence from algal gyttja to low-organic clayey mud to reflect a gradient of decreasing OC (from 10–26% to 3–12%) and increasing BSi (10–

Table 1. AMS  $^{14}\text{C}$  dates on core NC93.2-L from Crescent Island Crater in Lake Naivasha, Kenya. Calendar yrs (and ranges) listed are the intercepts ( $\pm 1 \sigma$ ) of the  $^{14}\text{C}$  dates with the bidecadal calibration curve (Stuiver & Reimer, 1993)

| Lab no.    | Depth (cm) | Dated material                       | $^{14}\text{C}$ yr BP | $\delta^{13}\text{C}$ PDB | Cal yr AD ( $\pm 1 \sigma$ )                         |
|------------|------------|--------------------------------------|-----------------------|---------------------------|--|
| CAMS 39312 | 150–178    | grass charcoal                       | 120 $\pm$ 50          | –25‰                      | 1702, 1718 (1680–1753); 1819, 1860, 1917 (1803–1937) |
| CAMS 39314 | 350–374    | <i>Acacia</i> leaves, grass charcoal | 320 $\pm$ 40          | –25‰                      | 1530, 1537, 1635 (1511–1647)                         |
| CAMS 39315 | 374–398    | grass charcoal                       | 480 $\pm$ 50          | –25‰                      | 1436 (1414–1449)                                     |
| CAMS 18702 | 419–420    | sedge rhizome                        | 580 $\pm$ 40          | –12‰                      | 1400 (1314–1411)                                     |
| CAMS 39316 | 486–506    | <i>Acacia</i> leaves, grass charcoal | 770 $\pm$ 50          | –25‰                      | 1278 (1229–1288)                                     |
| CAMS 39317 | 506–510    | <i>Acacia</i> twig                   | 930 $\pm$ 50          | –25‰                      | 1052, 1085, 1121, 1139, 1156 (1028–1178)             |
| CAMS 39318 | 538–542    | charred wood                         | 820 $\pm$ 50          | –25‰                      | 1229 (1191–1278)                                     |
| CAMS 32028 | 542–546    | wood                                 | 1100 $\pm$ 60         | –25‰                      | 910, 906 (892–930); 982 (938–1000)                   |
| CAMS 39319 | 558–562    | unburned grass stem                  | 1250 $\pm$ 50         | –12‰                      | 779 (689–873)  |
| CAMS 39321 | 562–566    | wood, bark, <i>Acacia</i> leaf       | 1030 $\pm$ 50         | –25‰                      | 1014 (983–1029)                                      |
| CAMS 39320 | 562–566    | sedge rhizome                        | 1040 $\pm$ 50         | –12‰                      | 1011 (978–1026)                                      |
| CAMS 22972 | 592–602    | grass charcoal                       | 1140 $\pm$ 60         | –25‰                      | 890 (869–985)  |
| CAMS 39322 | 754–774    | sedge rhizome                        | 1490 $\pm$ 50         | –12‰                      | 600 (544–636)  |
| CAMS 39323 | 806–822    | grass charcoal                       | 1800 $\pm$ 50         | –25‰                      | 239 (214–262)  |

18% to 22–30%). High-carbonate clayey mud is characterized by high IC (1.4–3.2%) and low BSi (8–12%) values. Silty peat differs from organic clayey mud by its coarse texture and by a substantial portion (15%) of the OC being plant fragments  $> 250 \mu\text{m}$ . The diatom-rich layers have low OC (4–14%) and high to very high BSi (22–58%) values.

Four of these seven sediment types were deposited in the center of Crescent Island Crater and/or Lake Oloidien at some time during the historical period, AD 1883 to present (Figure 4). Clayey mud was deposited in Crescent Island Crater during the periods of low to intermediate lake level before 1890 and after 1940 (Units I and III). Organic clayey mud was deposited both in Crescent Island Crater and Lake Oloidien during the period of high lake level from 1890 to 1940 (Unit II), except that in the former basin it is interrupted at 98–102 cm depth by a section of algal gyttja. This gelatinous and extremely fine-grained facies reflects a hemipelagic sedimentation regime with little or no influence from shallow-water environments. Its occurrence in Crescent Island Crater coincides with a short period in the early 1900s when total lake depth exceeded 25 m (Figure 4), high enough for the normally shallow and wind-stressed northeast sector of Lake Naivasha (Figure 1) to deposit fine-grained sediments locally and thus stop contributing to profundal sedimentation in the crater (Verschuren, 1999a). Renewed clastic input into the crater, reflected by the stratigraphic transition to organic clayey mud at 98 cm, was probably initiated by lake-level decline between 1906 and 1910. In Lake Oloidien, low and intermediate lake levels

before 1890 and after 1940 are represented by high-carbonate clayey mud (Units I and III). Sedimentary evidence for  $\text{CaCO}_3$  precipitation in the hydrologically closed basin of Lake Oloidien is consistent with field data indicating high pH (9.0–9.2), a low dissolved Ca/Na ratio compared to Lake Naivasha, and supersaturation with regard to calcite (Gaudet & Melack, 1981). By contrast, the low-carbonate sediments of Unit II were deposited when Lake Oloidien was broadly confluent with Lake Naivasha (cf. line 1 in Figure 4) and fresh (Beadle, 1932; Verschuren et al., 1999).

In Crescent Island Crater, and to a lesser extent in Lake Oloidien, OC (or OM) content of recent sediments is positively correlated with lake depth at the time of deposition (Figure 5, left panels). Negative correlation between OM and  $^{210}\text{Pb}$ -inferred sedimentation rates in both lakes (Figure 5, right panels) suggests that this may arise primarily because of depth-controlled variation in the dilution of autochthonous (algal) OM with minerogenic sediment components, rather than variation in OM production or preservation. This relationship can be explained as follows. In lake systems where peripheral wave action is responsible for most sediment redistribution (Hilton, 1985), and the mud-deposition boundary depth (Rowan et al., 1992; = critical depth *sensu* Håkanson, 1977) remains constant while lake level fluctuates, a lowering of lake level will move the lateral boundary between erosion and accumulation farther offshore, so that oxidized (low-organic) shallow-water sediments are focused into an increasingly smaller zone of undisturbed deposition.

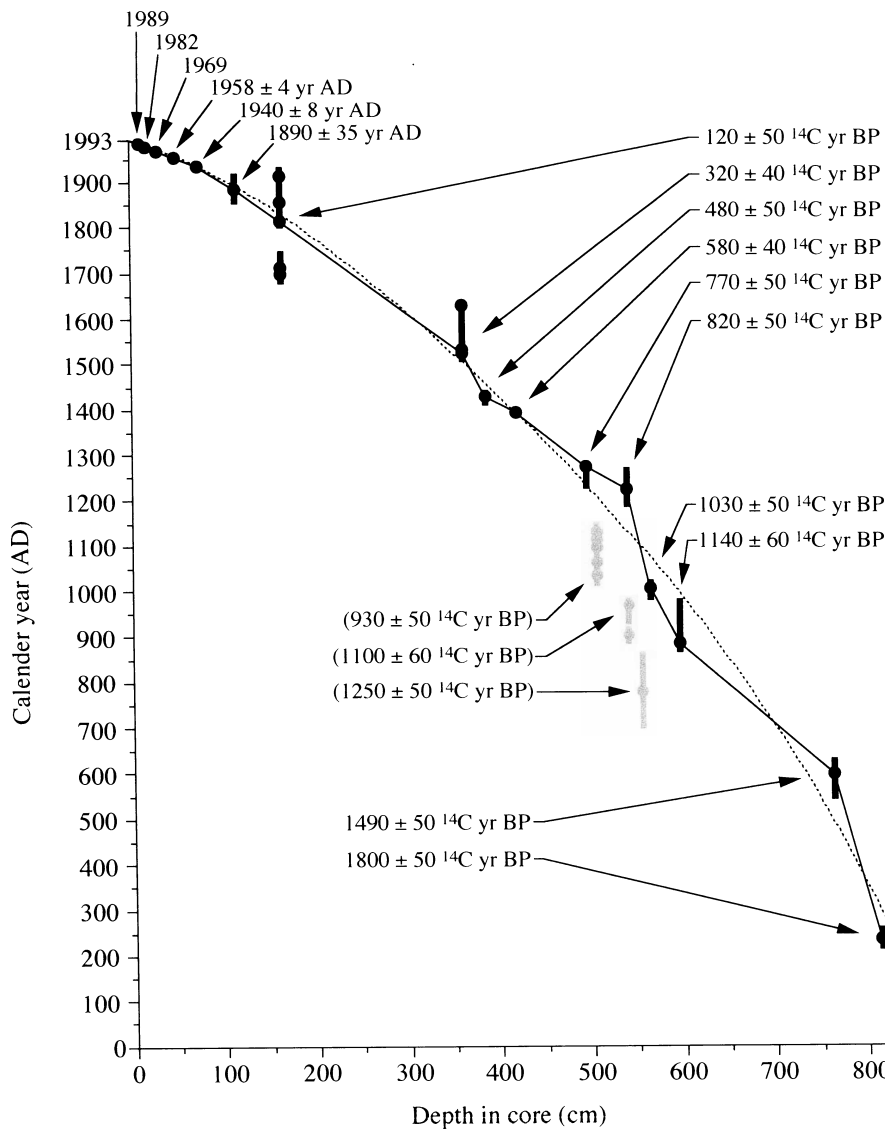


Figure 2. Composite  $^{210}\text{Pb}$  and  $^{14}\text{C}$  chronology of late-Holocene deposits in the Crescent Island Crater basin of Lake Naivasha. Filled symbols are the age of historical and correlational marker horizons (1890–1989), or the calendar-age solutions (vertical bars:  $\pm 1 \sigma$ ) of  $^{14}\text{C}$ -dated sediment intervals (pre-20th century, cf. Table 1). The solid line shows the depth-age relationship in an age model based on linear interpolation, the dashed line an age model based on 4th-order polynomial regression of all the marker horizons and the  $^{14}\text{C}$  dates shown in black.

Thus, the positive relationship between OM content and lake depth results from the negative relationship between lake depth and clastic input per unit area of the accumulation zone.

Low-organic clayey mud (Figure 3) has not been deposited in central areas of Crescent Island Crater or Lake Ololdien during historical times, but is common in older deposits of Crescent Island Crater. I interpret this facies to mainly reflect further dilution of autochthonous OC by clastic input (Dean & Gorham, 1976) at lake

depths shallower than have occurred over the past 115 yrs. Enhanced microbial degradation of OM due to repeated resuspension in a wind-stressed shallow lake environment may be co-responsible for the low OC values, as suggested by the relatively high BSi to OC ratio. In either case, the stratigraphic occurrence of low-organic clayey mud must reflect lowstand conditions during which the surface elevation of Crescent Island Crater stood below the sill connecting it to Lake Naivasha. Shallow conditions are also usually inferred

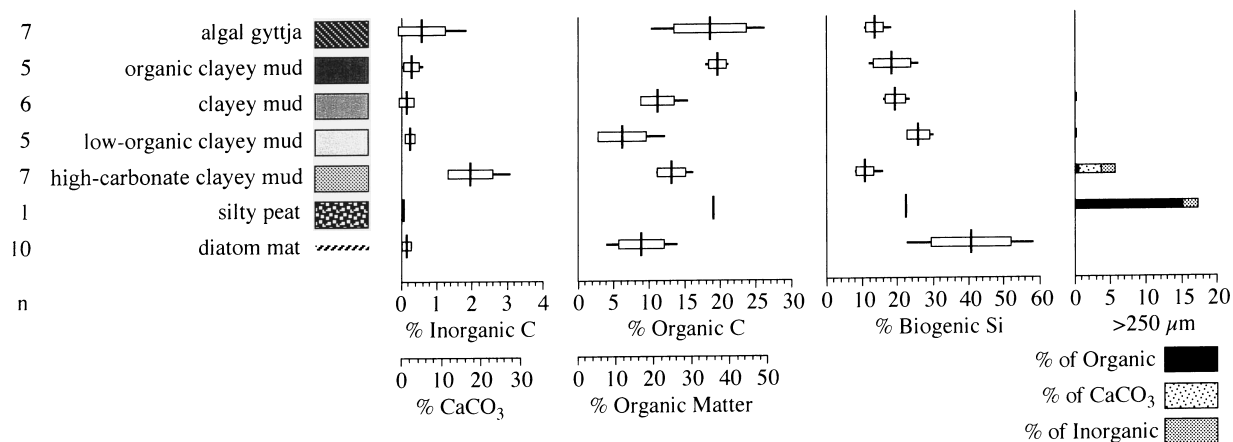


Figure 3. Mean  $\pm$  1 S.D. and range of the fractions of inorganic C and  $\text{CaCO}_3$ , organic C and organic matter, biogenic Si, and the average percentage of each fraction consisting of  $> 250 \mu\text{m}$  particles, for each of the seven major sediment types distinguished in core description; n = number of samples.

(Digerfeldt, 1986; Dearing, 1997) from the stratigraphic occurrence of silty or sandy peat (Figure 3), which in the Crescent Island Crater record occurs only in a single horizon at 146–150 cm core depth. It reflects an episode when submerged weed-beds grew across the bottom of the crater basin ( $< 5 \text{ m}$  depth) and the main basin of Lake Naivasha stood dry. Abundant remains of *Ceratophyllum demersum* indicate persistence of freshwater conditions despite this strong draw-down. In contrast, high-carbonate clayey mud is a lowstand facies (Dean & Gorham, 1976) that reflects the biogenic precipitation of  $\text{CaCO}_3$  following evaporative concentration of dissolved salts, as occurs in Lake Oloidien today. The stratigraphic occurrence of high-carbonate mud in the Crescent Island Crater record defines lowstands when the crater functioned as a hydrologically closed basin, i.e. when evaporative concentration exceeded solute removal through subsurface outflow.

Centimeter-scale diatom layers resembling the distinct horizons in core NC93.2-L (Figure 6a) have previously been described for marine settings (Kemp & Baldauf, 1993), and interpreted to reflect rapid mass sinking of live diatom cells (Smetacek, 1985). In the Crescent Island Crater record most layers consist of mono-specific flaky aggregates (1–3 mm across) of the planktonic diatom *Synedra acus* var. *radians* (Figures 6b & 6c). Their relative purity and sharp stratigraphical boundaries, along with an upward decrease of median flake size within each layer (Figure 6a), indicate that they do indeed represent short-lived events of rapid

deposition, i.e. several orders of magnitude faster than the long-term average rate of sediment accumulation. The low incidence of frustule damage (cf. Figure 6c) seems to argue for direct settling from the water column. However, if these layers were formed by mass sinking of live *Synedra*, the number of diatoms contained in a typical layer (equivalent to deposition of  $\sim 275 \times 10^6 \text{ cells cm}^{-2}$ ) would imply a pre-sinking average density of  $\sim 500 \times 10^3 \text{ cells mL}^{-1}$  in the 5-m-tall photic zone of Crescent Island Crater, which is two orders of magnitude higher than normally observed in diatom blooms (Round, 1981). Alternatively, the mats may have been deposited after selective winnowing of fossil *Synedra* frustules from soft surficial sediments becoming subject to wind-driven resuspension during lake-level decline. Resuspension events in Lake Naivasha could potentially entrain massive quantities of these needle-shaped diatoms, which would naturally entangle to form flaky aggregates and settle from suspension in the quiet deep basin of Crescent Island Crater. Primary association of the diatom mats with clayey mud (14 out of 18 occurrences) supports the deduction that mat formation is promoted within the range of lake depths when the crater is confluent with a shallow Lake Naivasha (Verschuren, 1999a). The diatom mats in sections of low-organic clayey mud and high-carbonate clayey mud (2 occurrences each) must then have resulted from secondary reworking of older deposits during extreme lowstands. *Synedra acus* was a common species in Lake Naivasha phytoplankton between about 1910 and the 1940s (K. R. Laird,

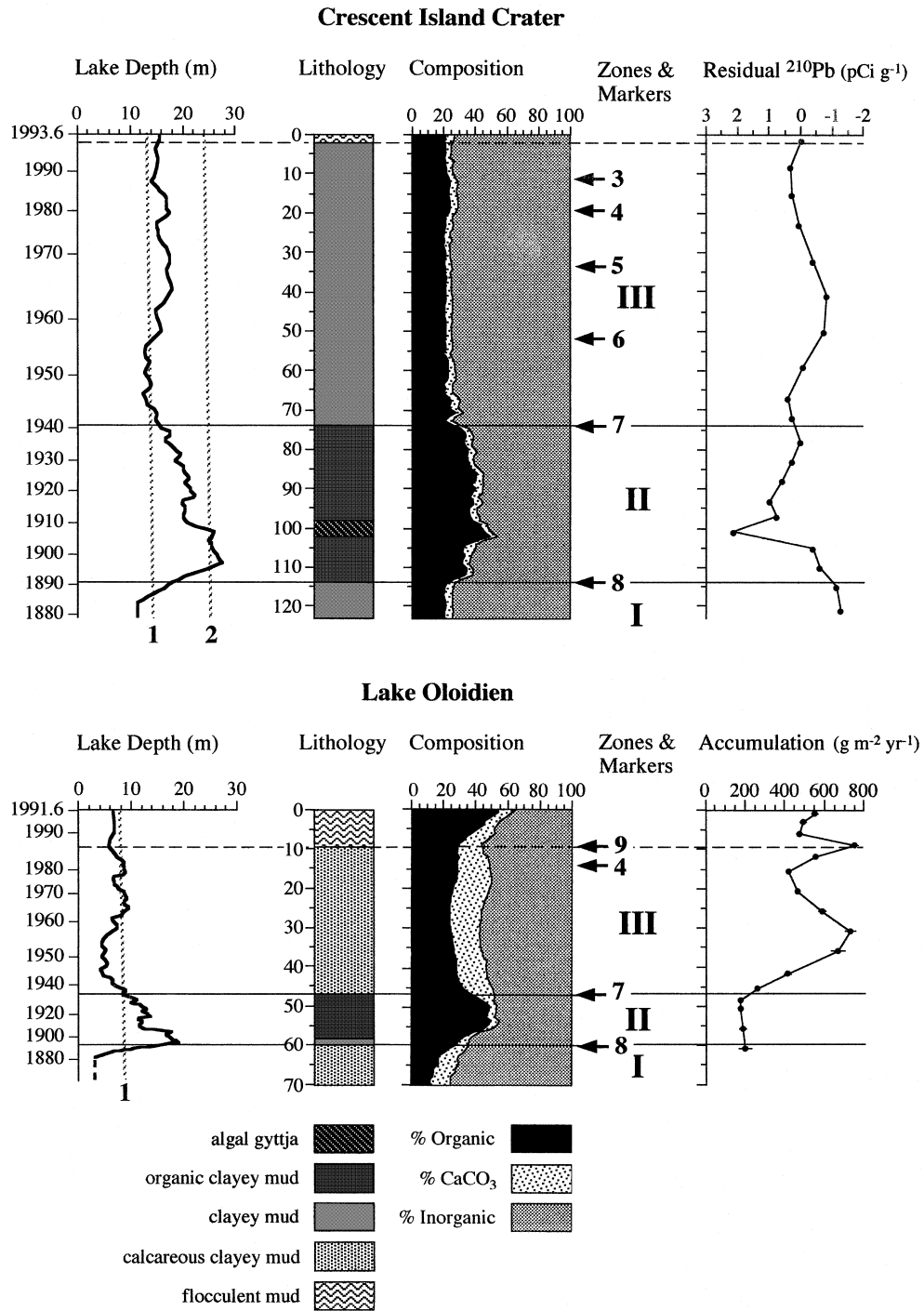


Figure 4. Composition, stratigraphic zones, and accumulation rate of sediments in Crescent Island Crater (core NC93.1-S, top) and Lake Oloidien (core NO91.1-S, bottom) during the historical period in relation to lake depth at the time of deposition (full line), Lake Naivasha sill elevation (stippled line 1), and the elevation at which Crescent Island Crater stops functioning as a sediment trap for the northeast sector of Lake Naivasha, as predicted by wave theory (stippled line 2). Sediment chronology is anchored in six (Crescent Island Crater) and four (Oloidien) historical or correlative marker horizons, including documented outbreaks of the water fern *Salvinia molesta* (3–5), peak *Daphnia longispina* abundance (6), the top and bottom boundary of Unit II (7, 8), and peak sediment accumulation during the 1988 lowstand (9; see Verschuren, 1999a; Verschuren et al., 2000). In core NC93.1-S, residual <sup>210</sup>Pb activity is used as a proxy for accumulation rate. Flocculent surface muds are omitted from analyses of the relationship between lake depth and sedimentation.

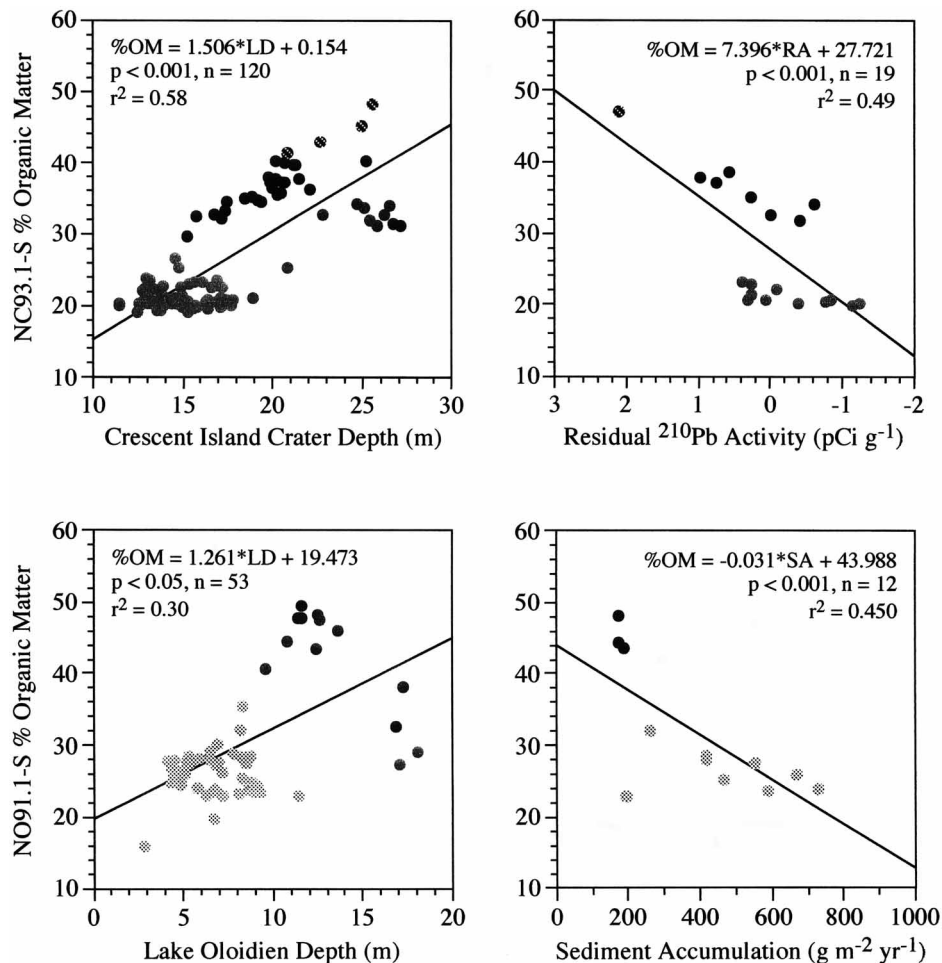


Figure 5. Relationships between organic-matter (OM) content and lake depth (LD), and between organic-matter content and sediment accumulation (SA, or its proxy, the residual activity of  $^{210}\text{Pb}$ , RA), in Crescent Island Crater (core NC93.1-S, top) and Lake Oloidien (core NO91.1-S, bottom) during the historical period. Symbols follow the key to lithology in Figure 4.

unpublished data), but the lack of well-defined diatom mats in the historical sediment record suggests that conditions favorable to their formation have not occurred.

#### *Lake-level history of Crescent Island Crater*

Pre-20th century deposits in Crescent Island Crater comprise seven sedimentary units (Figure 7) which following Verschuren (1999a) are here labeled as sub-units a-g of Unit 0. Corer penetration beyond 822 cm was prevented by stiff sediments deposited before  $1800 \pm 50$   $^{14}\text{C}$  yr BP. Richardson & Richardson (1972) encountered a hard sandy layer at about 8 m sediment depth, and interpreted it to be a soil horizon formed at a time when the crater basin stood dry. The conventional

date of  $3040 \pm 60$   $^{14}\text{C}$  yr BP cited by these authors for bulk OC from lake muds overlying the stiff soil horizon may overestimate its true age because of carbon-isotope fractionation in evaporating lake water, or groundwater exchange with geological carbonates (Fontes, 1992).

Sub-units 0g (822–710 cm) and 0f (710–572 cm) are composed of clayey muds, low-organic clayey muds, and high-carbonate clayey muds representing the period of lake filling after AD 200 followed by a regime of low to intermediate lake depths until AD 1000. Sub-unit 0e (572–506 cm) consists of two massive horizons of high-carbonate clayey mud separated by a 12-cm section of low-organic clayey mud and clayey mud. High-carbonate muds in the horizon 572–544 cm occur together with  $^{14}\text{C}$  evidence for physical reworking of older deposits and low net sediment accumulation

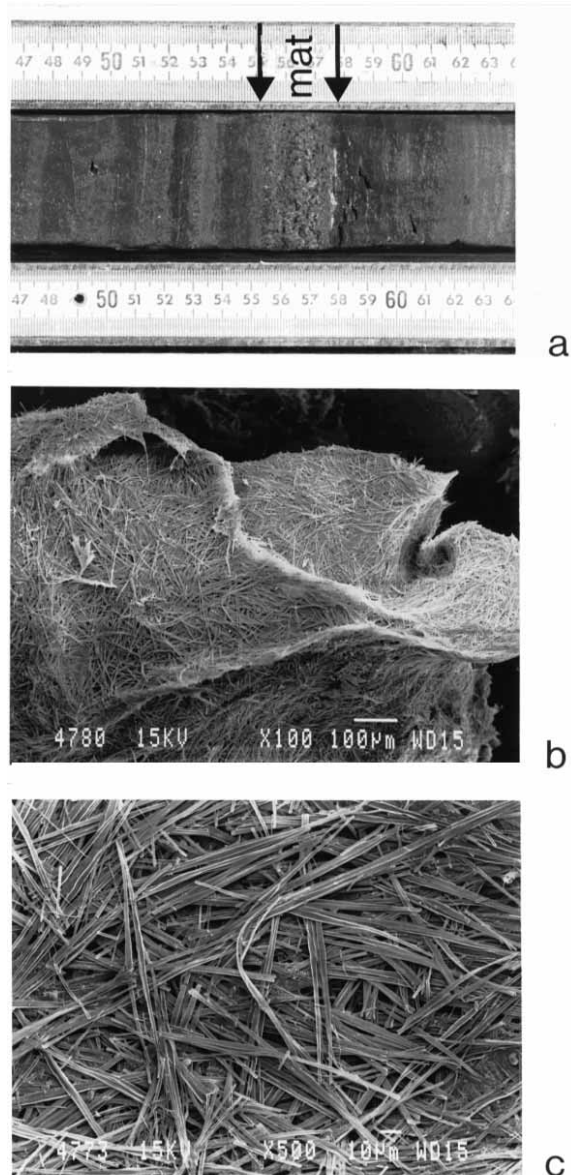


**Figure 6.** Stratigraphic appearance and texture of the diatom mats. (a) Cross section of the 2.5-cm thick diatom mat at 709.5–712 cm depth (delimited by black arrows; core top is to the left) showing pale-colored diatom flakes and the upward reduction in flake size; (b) S.E.M. top view of a single flake from near the bottom of the diatom mat; (c) Detail of flake surface showing mono-specific aggregates of the planktonic diatom *Synedra acus* var. *radians*.

(Figure 2), indicating a prolonged lowstand with lake depths possibly as low as 2–3 m during the period AD 1000–1200. Following a brief interlude of positive water balance in the early 13th century, resumption of massive  $\text{CaCO}_3$  precipitation reflects another lowstand during AD 1230–1270.

Sub-unit 0d (506–348 cm) recorded at least two cycles of rising and falling lake level between about AD 1270 and 1580. Sedimentological evidence suggests a generally positive water balance from AD 1270 until the late 15th century, interrupted by one return to hydrological closure around AD 1400. Except for the high-carbonate clayey mud deposited during this inferred lowstand, much of sub-unit 0d consists of clayey muds and organic clayey muds reflecting lake depths within the range of 20th-century fluctuations and a probable highstand (lake depth 20–25 m) in the second half of the 15th century. This highstand ended in the early 16th century with a period of strong lake-level decline to a pronounced late-16th-century lowstand represented by the 16-cm thick section of high-carbonate clayey mud at the base of Sub-unit 0c (348–258 cm). Transition to low-organic clayey mud above this section is interpreted to reflect stabilization of lake level and a temporary switch to positive water balance around AD 1600, followed by one more fall below the Lake Naivasha sill.

The transition to massive clayey mud at 302 cm and progressive increase of OM content in the upper half of Sub-unit 0c suggests that Crescent Island Crater recovered from the late-16th-century lowstand with a steady rise in lake level starting around AD 1620 and continuing throughout the 17th century. Eventual transition from organic clayey mud to algal gyttja (Figure 7) reflects the onset of hemipelagic sedimentation initiated by complete isolation of the crater basin from source areas of coarse-grained mineral input. The extremely porous and gelatinous texture of Sub-unit 0b algal gyttja (258–198 cm) as compared to that deposited around 1900 (Figure 4) suggests that lake level may have stood well above the historical maximum of 1897 m a.s.l. reached in 1894. If lake depth exceeded 30 m, also the island now forming the west and south rim of Crescent Island Crater (Figure 1) would have largely disappeared below the water surface. Interpolation between available  $^{14}\text{C}$  dates (Figure 2) places this major highstand to between about AD 1680 and 1770.

Sub-unit 0a (198–144 cm) recorded the strong lake-level decline that ensued. Algal gyttja above the 0b–0a boundary is clayey rather than gelatinous, and its OM content declines (Figure 7). At 170 cm the gyttja changes to high-carbonate clayey mud, followed at 162 m by low-organic clayey mud. This stratigraphic sequence reflects a suite of events in which Crescent Island Crater first started to again receive coarse-grained material from the increasingly wind-stressed

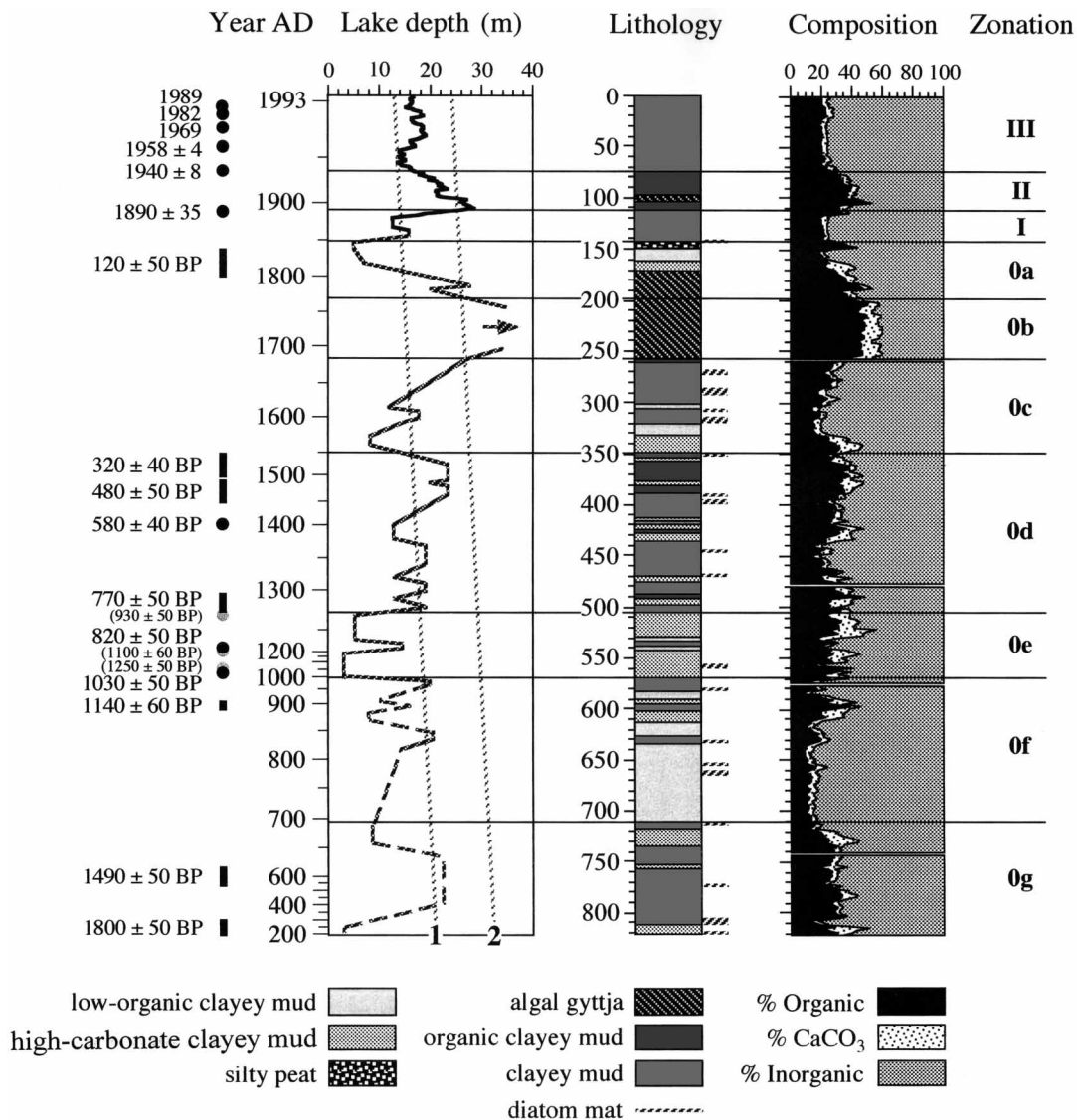


Figure 7. Chronology and sedimentology-inferred lake-level reconstruction for Crescent Island Crater over the past 1800 yrs; reconstruction before 1000 AD is tentative. Stippled lines 1 and 2 represent the Lake Naivasha sill elevation, and the elevation at which Crescent Island Crater stops functioning as a sediment trap for the northeast sector of Lake Naivasha, as in Figure 4.

bottom of Lake Naivasha, until around AD 1800 lake level dropped below the crater rim and the northeast sector of Lake Naivasha fell dry. Further drawdown culminated in deposition of the silty peat at the top of Sub-unit 0b, testimony to a brief episode about AD 1830–1840 when Lake Naivasha fell completely dry and Crescent Island Crater was so shallow (< 5 m) that submerged macrophytes grew across the crater floor. Sub-unit 0a is overlain by the clayey muds of Unit I, deposited during the mid-19th century episode of renewed lake filling and intermediate levels

(Verschuren, 1999a) that preceded the historically documented transgression of the 1880s–1890s (Åse et al., 1986).

## Discussion

### Chronology

The fairly even distribution of radiometric dates on a plot of sediment age vs. depth (Figure 2) suggests that

the floor of Crescent Island Crater enjoyed continuous sedimentation since  $1800 \pm 50$   $^{14}\text{C}$  yr BP, or about AD 240. Over the past 1800 yrs, linear sediment accumulation in Crescent Island Crater has averaged  $4.7 \text{ mm yr}^{-1}$ . Reduced accumulation prior to  $1490 \pm 50$   $^{14}\text{C}$  yr BP and between  $1030 \pm 50$  and  $770 \pm 50$   $^{14}\text{C}$  yr BP may reflect episodic interruption of local accumulation and the reworking of older deposits at low lake level (Whitmore et al., 1996; Verschuren, 1999a). Three out-of-sequence  $^{14}\text{C}$  dates ( $930 \pm 50$ ,  $1100 \pm 60$ , and  $1250 \pm 50$   $^{14}\text{C}$  yr BP; Table 1) on single macrofossils recovered from high-carbonate clayey mud between 506 and 572 cm are omitted from the chronology on the basis that they may be derived from such reworked deposits. Accelerated sedimentation after 1900 is due partly to incomplete compaction of recent sediments and partly to increased clastic input from disturbed soils in the Malewa River drainage since European settlement (Harper et al., 1990). The accuracy of the Crescent Island Crater record as an archive of climate history is constrained by the analytical uncertainty associated with  $^{14}\text{C}$ -based age determination and additional uncertainty due to the occurrence of non-unique calendar ages. An alternative age model based on polynomial regression rather than linear interpolation of the  $^{14}\text{C}$  data (Figure 2) accounts for this uncertainty better but does not properly reflect the apparently real changes in sedimentation rate through time, such as the reduced accumulation (Figure 2) during the inferred lowstand of AD 1000–1200 (Figure 7).

#### *Depth inference from sediment composition*

This reconstruction of past lake-level fluctuations in Crescent Island Crater relies to a large extent on historical calibration of the influence of lake depth and hydrological closure on sediment composition. Positive correlation between sedimentary OC and lake depth is due to depth dependence in the rate of clastic dilution (Figure 5), while high-carbonate clayey mud and algal gyttja are the sedimentological consequences of hydrological closure and a shutdown of clastic input. In this sense, this sedimentology-inferred lake-level reconstruction is akin to the reconstruction of alpine glacier activity from variations in the OC content of downvalley lake sediments (Leonard, 1986; Souch, 1994). In shallow fluctuating lakes considered here, valid extrapolation of a historical relationship between OC concentration and lake depth to older deposits depends on lake depth exerting dominant control on the rate of clastic dilution, and clastic dilution exerting dominant control on OC

concentration. The first assumption may be violated for modest or short-lived fluctuations, where transient sedimentation dynamics may be important (Verschuren, 1999b). For example, in Lake Oloidien and to lesser extent also in Crescent Island Crater, the relationship between OC concentration and lake depth is subject to hysteresis, with OM values being relatively lower during lake-level rise than during decline (Figure 5). Likely, this is due to transient dynamics and threshold effects, for example a temporary rise of clastic influx following the inundation of exposed peripheral mudflats. The second assumption may have been violated during extreme lowstands due to discontinuous sedimentation (Whitmore et al., 1996; Verschuren, 1999b), enhanced OC oxidation on a wind-stressed lake floor (Talbot & Allen, 1996), or because changes in the hydrological balance affected nutrient cycling and algal productivity (Harper et al., 1993). Because the relationship between OC and lake depth also depends on the relationship between sedimentation and basin morphometry, it must have been modified over time by natural basin infilling. In Crescent Island Crater, this amounts to 25% of the total range of inferred lake depths over the past 1800 yrs. Hence it can not be assumed negligible. Because of these complicating factors, historical calibration of sediment composition may have little bearing on the oldest part of the sediment record, particularly that from before the AD 1000–1200 lowstand.

Another potential problem concerns inference of lowstands from the stratigraphic distribution of low-organic clayey mud and high-carbonate clayey mud. It is possible that thick horizons of low-organic clayey mud, such as those at 634–710 cm and 302–322 cm, do not reflect increased clastic input and/or OC oxidation during a lowstand, but massive influx of oxidized muds when previously exposed Lake Naivasha mudflats were flooded in the course of a major transgression. In that case, low-organic clayey mud would represent the recovery from a lowstand rather than the lowstand itself. Also, although high-carbonate muds are characteristic for shallow closed-basin lakes (Dean & Gorham, 1976), they are an imprecise indicator of lake depth because initiation of  $\text{CaCO}_3$  precipitation will depend on a basin's previous history of solute accumulation and removal. In this study, high-carbonate mud is assumed to reflect effective hydrologic closure or, at least, a rate of evaporative concentration greater than the rate at which salts are removed through subsurface outflow. Historical conductivity data suggest that true hydrologic closure of Crescent Island Crater requires drawdown to well below the Lake Naivasha sill, possibly even the complete

desiccation of Lake Naivasha (cf. Figure 1). Such conditions must have prevailed during deposition of the massive sections of high-carbonate clayey mud representing the lowstands of AD 1000–1270, 1380–1400, and 1560–1590. Some admixture of coarse sand and marl in these core sections (Figure 3) is consistent with proximity to a high-energy littoral environment. Intermittent episodes of rapid evaporative concentration may occasionally have triggered  $\text{CaCO}_3$  precipitation without true hydrologic closure of the crater basin, which would explain some minor horizons of high-carbonate mud bedded between other facies. For example, lithological evidence for the AD 1760–1840 lowstand includes only a thin section of high-carbonate mud, despite the fact that Crescent Island Crater at this time may have reached its lowest level since AD 1200. Abundant *Ceratophyllum* fossils in the silty peat deposited at that time clearly indicates that the crater survived early-19th century aridity as a fresh weedy pond. Likely, the 150-yr period of confluence with Lake Naivasha immediately before this draw-down completely flushed the system of the salts that had accumulated during earlier episodes of negative water balance.

#### *Comparison with other climate-proxy records*

Despite the uncertainties discussed above, mechanistic interpretation of sediment composition appears to have yielded a coherent and eventful history of climate-driven lake-level fluctuations in the Lake Naivasha system with decade- to century-scale resolution. Historical data bearing on the climatic significance of pre-20th century fluctuations are mostly limited to the early-19th century lowstand and the preceding highstand. Stratigraphic evidence for a pronounced lowstand from about AD 1800–1840 agrees with historical sources indicating severe aridity in East Africa from the late 1700s to the 1820s–1830s, followed by a return to wetter conditions by the mid-19th century (Nicholson, 1995). While Crescent Island Crater survived this arid interval as a shallow pond, desiccation surfaces and other evidence for discontinuous sedimentation beneath 19th-century lake muds in Lake Naivasha, Lake Oloidien, and Lake Sonachi show that these shallower basins fell completely dry (Verschuren, 1999a, b; Verschuren et al., 1999). Desiccation of shallow lakes at that time was widespread, as testified by the stiff low-organic clays underlying a few decimeters of organic muds in many Kenyan Rift lakes, such as Lakes Nakuru and Elmenteita (Richardson & Dussinger, 1986), Lake Baringo (Barton et al., 1987),

and Lake Bogoria (Tiercelin et al., 1987).

Stratigraphic evidence for an extraordinary highstand of Lake Naivasha during the period AD 1680–1770 agrees with records of pre-19th century highstands at Lake Turkana in northern Kenya (Halfman et al., 1994), Lake Chad in the Sahel (Maley, 1976), and Lake Chilwa in Malawi (Crossley et al., 1984). At Lake Chilwa, the age of trees growing below a raised shoreline dated to  $160 \pm 50$   $^{14}\text{C}$  yr BP constrains the end of this highstand to shortly before AD 1760, a close match with the Crescent Island Crater chronology. Starting out from the late-16th-century lowstand, this highstand evidently resulted from increased rainfall dated in Crescent Island Crater to between AD 1625 and 1750 (Figure 7). Thus, equatorial East Africa must have enjoyed a significantly wetter climate than today during the second half of the LIA, coeval with greatest LIA cooling in Europe (Bradley & Jones, 1993). During the first half of the LIA, from about AD 1270–1620, the Lake Naivasha area enjoyed a mostly positive water balance punctuated by arid spells dated to AD 1380–1400 and AD 1560–1590 (Figure 7). Not much information from elsewhere in Africa exists to compare these data with. The Lake Turkana record (Halfman et al., 1994) lacks detail in this period, and Lake Chad (Maley, 1976) appears to have stood low through most of early LIA time but also here chronological control is poor. During the period AD 1000–1270, coincident with positive temperature anomalies in Europe and South Africa identified as the MWP (e.g. Tyson & Lindesay, 1992), Crescent Island Crater experienced a prolonged lowstand. No dated sediment records from other small lakes cover this period, but those from the large Rift Lakes Turkana, Tanganyika, and Malawi all agree with the Crescent Island Crater record in suggesting a relatively dry climate during that time.

The apparent lack of stratigraphic evidence for a pronounced LIA-period highstand in other African lake-sediment records is notable. In shallow lakes of the Kenya Rift that are known to have fallen dry in the early 19th century, organic lake muds just beneath the desiccation surface, or remnants of reworked lake muds incorporated into the desiccation horizon, all have AMS  $^{14}\text{C}$  ages dating to before the AD 1680–1770 highstand: 290  $^{14}\text{C}$  yr BP in Lake Naivasha (Verschuren, 1999a), 375  $^{14}\text{C}$  yr BP in Lake Bogoria (M. R. Talbot, personal communication), and 520  $^{14}\text{C}$  yr BP in Lake Sonachi (Verschuren, 1999b). Without knowledge of the complete Crescent Island Crater record nearby, truncation of sediment records during the 19th-century drystand would have appeared to reflect a much earlier onset of

aridity than actually occurred, and mistakenly create the impression that East Africa was dry during much of the LIA. Similarly, a massive horizon of stiff silty clays underlying 19th-century muds in Lake Chiuta suggests 'a long-lasting dry phase prior to AD 1850' (Owen & Crossley, 1989), but sediments from below the desiccation horizon that could constrain the onset of aridity have not been sampled. Sediments underlying the sublacustrine erosion surface inferring a major LIA-period drawdown of Lake Malawi (Owen et al., 1990) also remain undated; the proposed date of AD 1500 for the start of this draw-down is based on a hiatus in the archaeological record of fishing villages on the present-day shoreline. Other studies inferring prolonged LIA aridity (Bonnefille & Mohammed, 1994; Stager et al., 1997) lack sufficient time control to permit confidence that the climate-proxy record is continuous and/or that core tops reflect modern sedimentation. The combined evidence from those records that have adequate time control is consistent with the inference from Crescent Island Crater history that tropical East Africa was drier than today during the Medieval Warm Period, and significantly wetter than today during the second half of the Little Ice Age.

### Acknowledgments

This work was supported by NSF-DEB 93-20324, NSF-ATM 95-31222, NSF-RTG 90-14277, and the Quaternary Paleocology program at the University of Minnesota. The field campaign was conducted with permission from the Office of the President of the Republic of Kenya to K. Mavuti. I thank the Lake Naivasha Riparian Association for lake access, K. Mavuti, B. Ammann, H. E. Wright, and F. Janssen for help in the field, D. Engstrom for access to  $^{210}\text{Pb}$ -dating facilities, H. Segers for access to S.E.M., C. Cocquyt for quantitative diatom data, and K. Kelts, K. Laird, J. Smoot, and M. Talbot for constructive comments on the manuscript. The author acknowledges pre-doctoral fellowships from the Belgian-American Educational Foundation and the Graduate School of the University of Minnesota, and is currently post-doctoral fellow with the Fund for Scientific Research of Flanders (Belgium). This work also benefited from a National Oceanic and Atmospheric Administration post-doctoral fellowship in Climate and Global Change Research at the Large Lakes Observatory, University of Minnesota. This is Limnological Research Center contribution 536.

### References

- Appleby, P. G. & F. Oldfield, 1978. The calculation of lead-210 dates assuming a constant rate of supply of unsupported  $^{210}\text{Pb}$  to the sediment. *Catena* 5: 1–8.
- Åse, L.-E., K. Sernbo & P. Syrén, 1986. Studies of Lake Naivasha, Kenya, and its drainage area. *Forskningsrapp. Naturgeogr. Inst. Stockholms Univ.* 63: 1–75.
- Barton, C. E., D. K. Solomon, J. R. Bowman, T. E. Cerling & M. D. Sayer, 1987. Chloride budgets in transient lakes: lakes Baringo, Naivasha, and Turkana. *Limnol. Oceanogr.* 32: 745–751.
- Beadle, L. C., 1932. Scientific results of the Cambridge expedition to the east African lakes, 1930–1931. 4. The waters of some East African lakes in relation to their fauna and flora. *J. Linn. Soc. (Zool.)* 38: 157–211.
- Bonnefille, R. & U. Mohammed, 1994. Pollen-inferred climatic fluctuations in Ethiopia during the last 3000 yrs. *Palaeogeogr. Palaeoclimatol. Palaeoecol.* 109: 331–343.
- Bradley, R. S. & P. Jones, 1993. 'Little Ice Age' summer temperature variations: their nature and relevance to recent global warming trends. *Holocene* 3: 367–376.
- Cohen, A. S., M. R. Talbot, S. M. Awramik, D. L. Dettman & P. Abell, 1997. Lake level and paleoenvironmental history of Lake Tanganyika, Africa, as inferred from late Holocene and modern stromatolites. *Geol. Soc. Am. Bull.* 109: 444–460.
- Crossley, R., S. Davison-Hirschmann, R. B. Owen & P. Shaw, 1984. Lake-level fluctuations during the last 2,000 yrs in Malawi. In J. C. Vogel (ed.), *Late Cenozoic Palaeoclimates of the Southern Hemisphere*, Balkema, Rotterdam, 305–316.
- Darling, W. G., D. J. Allen & H. Armannsson, 1990. Indirect detection of subsurface outflow from a rift valley lake. *J. Hydrol.* 113: 297–305.
- Dean, W. E., 1974. Determination of carbonate and organic matter in calcareous sediments and sedimentary rocks by loss on ignition: comparison with other methods. *J. Sed. Petrol.* 44: 242–248.
- Dean, W. E. & E. Gorham, 1976. Major chemical and mineral components of profundal surface sediments in Minnesota lakes. *Limnol. Oceanogr.* 21: 259–284.
- Dearing, J. A., 1997. Sedimentary indicators of lake-level changes in the humid temperate zone: a critical review. *J. Palaeolim.* 18: 1–14.
- DeMaster, D. J., 1981. The supply and accumulation of silica in the marine environment. *Geochim. Cosmochim. Acta* 45: 1715–1732.
- Digerfeldt, G., 1986. Studies on past lake-level fluctuations. In B. E. Berglund (ed.), *Handbook of Holocene Palaeoecology and Palaeohydrology*. Wiley, New York, 127–143.
- Fontes, J.-Ch., 1992. Chemical and isotopic constraints on  $^{14}\text{C}$  dating of groundwater. In R. E. Taylor, A. Long & R. S. Kra (eds), *Radiocarbon After 4 Decades: An Interdisciplinary Perspective*. Springer, New York, 242–261.
- Gaudet, J. J. & J. M. Melack, 1981. Major ion chemistry in a tropical African lake basin, Freshwat. *Biol.* 11: 309–333.
- Håkanson, L., 1977. The influence of wind, fetch, and water depth on the distribution of sediments in Lake Vänern, Sweden. *Can. J. Earth Sci.* 14: 397–412.
- Håkanson, L., 1982. Lake bottom dynamics and morphometry – the dynamic ratio. *Wat. Resources Res.* 18: 1444–1450.
- Halfman, J. D., T. C. Johnson & B. P. Finney, 1994. New AMS

- dates, stratigraphic correlations and decadal climatic cycles for the past 4 ka at Lake Turkana, Kenya. *Palaeogeogr. Palaeoclimatol. Palaeoecol.* 111: 83–98.
- Harper, D. M., K. M. Mavuti & S. M. Muchiri, 1990. Ecology and management of Lake Naivasha, Kenya, in relation to climatic change, alien species' introductions, and agricultural development. *Envir. Conserv.* 17: 328–336.
- Harper, D. M., G. Phillips, A. Chilvers, N. Kitaka & K. Mavuti, 1993. Eutrophication prognosis for Lake Naivasha, Kenya. *Verh. Internat. Verein. Limnol.* 25: 861–865.
- Hilton, J., 1985. A conceptual framework for predicting the occurrence of sediment focusing and sediment redistribution in small lakes. *Limnol. Oceanogr.* 30: 1131–1143.
- Kemp, A. E. S. & J. G. Baldauf, 1993. Vast Neogene laminated diatom mat deposits from the eastern equatorial Pacific Ocean. *Nature* 362: 141–144.
- Leonard, E. M., 1986. Use of lacustrine sedimentary sequences as indicators of Holocene glacial activity, Banff National Park, Alberta, Canada. *Quat. Res.* 26: 218–231.
- MacIntyre, S. & J. M. Melack, 1982. Meromixis in an equatorial African soda lake. *Limnol. Oceanogr.* 27: 595–609.
- Maley, J., 1976. Les variations du lac Tchad depuis un millenaire: conséquences paleoclimatiques. *Palaeoecol. Afr.* 9: 44–47.
- Nicholson, S. E., 1995. Environmental change within the historical period. In A. S. Goudie, W. M. Adams & A. Orme (eds), *The Physical Geography of Africa*. Oxford University Press, Oxford, 60–75.
- Ojiambo, B. S. & W. B. Lyons, 1996. Residence times of major ions in Lake Naivasha, Kenya, and their relationship to lake hydrology. In T. C. Johnson & E. Odada (eds), *The Limnology, Climatology and Paleoclimatology of the East African Lakes*. Gordon & Breach, Newark, 267–278.
- Owen, R. B. & R. Crossley, 1989. Recent sedimentation in lakes Chilwa and Chiuta, Malawi. *Palaeoecol. Afr.* 20: 109–117.
- Owen, R. B., R. Crossley, T. C. Johnson, D. Tweddle, I. Kornfield, S. Davison, D. Eccles & D. R. Engstrom, 1990. Major low levels of Lake Malawi and their implications for speciation rates in cichlid fish. *Proc. Roy. Soc. Lond.* B240: 519–553.
- Richardson, J. L. & R. A. Dussinger, 1986. Paleolimnology of mid-elevation lakes in the Kenya Rift Valley. *Hydrobiologia* 143: 167–174.
- Richardson, J. L. & A. E. Richardson, 1972. History of an African Rift lake and its climatic implications. *Ecol. Monogr.* 42: 499–534.
- Round, F. E., 1981. *The ecology of algae*. Cambridge University Press, Cambridge.
- Rowan, D. J., J. Kalf & J. B. Rasmussen, 1992. Estimating the mud deposition boundary depth in lakes from wave theory. *Can. J. Fish. Aquat. Sci.* 49: 2490–2497.
- Smetacek, V. S., 1985. Role of sinking in diatom life-history cycles: ecological, evolutionary and geological significance. *Mar. Biol.* 84: 239–251.
- Souch, C., 1994. A methodology to interpret downvalley lake sediments as records of neoglacial activity: Coast Mountains, British Columbia, Canada. *Geogr. Ann.* 76A: 169–185.
- Stager, J. C., B. Cumming & L. Meeker, 1997. A high-resolution 11,400-yr diatom record from Lake Victoria, east Africa. *Quat. Res.* 47: 81–89.
- Stuiver, M. & P. J. Reimer, 1993. Extended <sup>14</sup>C data base and revised CALIB 3.0 <sup>14</sup>C age calibration program. *Radiocarbon* 35: 215–230.
- Talbot, M. R. & P. A. Allen, 1996. Lakes. In H. G. Reading (ed.), *Sedimentary Environments: Processes, Facies, and Stratigraphy*. Blackwell, Oxford, 83–124.
- Tiercelin, J. J. et al., 1987. Le demi-graben de Baringo-Bogoria, Rift Gregory, Kenya: 30.000 ans d'histoire hydrologique et sédimentaire. *Bull. Centr. Rech. Expl.-Prod. Elf-Aquitaine* 11: 249–540.
- Tyson, P. D. & J. A. Lindesay, 1992. The climate of the last 2000 yrs in southern Africa. *Holocene* 2: 271–278.
- Verschuren, D., 1993. A lightweight extruder for accurate sectioning of soft-bottom lake sediment cores in the field. *Limnol. Oceanogr.* 38: 1796–1802.
- Verschuren, D., 1996. Comparative paleolimnology in a system of four shallow, climate-sensitive tropical lake basins. In T. C. Johnson and E. Odada (eds), *The Limnology, Climatology and Paleoclimatology of the East African Lakes*. Gordon & Breach, Newark, 559–572.
- Verschuren, D., 1999a. Sedimentation controls on the preservation and time resolution of climate-proxy records from shallow fluctuating lakes. *Quat. Sci. Rev.* 18: 821–837.
- Verschuren, D., 1999b. Influence of lake depth and mixing regime on sedimentation in a small, fluctuating tropical soda lake. *Limnol. Oceanogr.* 44: 1103–1113.
- Verschuren, D., J. Tibby, P. R. Leavitt & C. N. Roberts, 1999. The environmental history of a climate-sensitive lake in the former 'White Highlands' of central Kenya. *Ambio* 28: 494–501.
- Verschuren, D., J. Tibby, K. Sabbe & C. N. Roberts, 2000. Effects of lake level, salinity and substrate on the invertebrate community of a fluctuating tropical lake. *Ecology*, 81: 164–182.
- Whitmore, T. J., M. Brenner & C. L. Schelske, 1996. Highly variable sediment distribution in shallow, wind-stressed lakes: a case for sediment-mapping surveys in paleolimnological studies. *J. Paleolim.* 15: 207–221.
- Wright, H. E. Jr., 1967. A square-rod piston sampler for lake sediments. *J. Sed. Petrol.* 37: 975–976.
- Wright, H. E. Jr., 1980. Coring of soft lake sediments. *Boreas* 9: 107–114.

